Second harmonic generation in modal phase-matched AlGaAs-on-insulator waveguides

Xinda Lu, *Yi* Zheng, *Chaochao* Ye, *Kresten* Yvind, and *Minhao* Pu*

DTU Electro, Department of Electrical and Photonics Engineering, Technical University of Denmark, 2800 Kgs. Lyngby, Denmark

Abstract. We utilize modal phase matching and type-I configuration to achieve second harmonic generation in AlGaAs-on-insulator waveguides. We demonstrate an overall normalized conversion efficiency of 200% W^{-1} cm^{-2} at a pump wavelength of 1587 nm in a 1-mm-long waveguide.

1 Introduction

Nonlinear frequency conversion processes play a pivotal role in advancing photonics technologies by enabling the generation of new optical frequencies through the interaction of light with nonlinear materials. Second harmonic generation (SHG) has garnered significant attention among these techniques. Materials with large second-order ($\chi^{(2)}$) nonlinearity are highly desired to realize efficient SHG. Aluminum gallium arsenide (AlGaAs) has been nominated as the "silicon of nonlinear optics" [1] as it offers both strong intrinsic second-order and third-order ($\chi^{(3)}$) nonlinearities. Tremendous efforts have been made to achieve efficient nonlinear processes (e.g., SHG and FWM) in AlGaAs waveguides [2]. However, the nonlinear performance is limited by the low optical confinement and the challenging deep etching process of the conventional AlGaAs waveguides. To obtain strong light confinement and relax the requirements of the patterning process, we have developed the AlGaAs-on-insulator (AlGaAsOI) platform [3], which emerged as a promising nonlinear platform for frequency conversion based on the $\chi^{(3)}$ [4], [5] and $\chi^{(2)}$ effects [6]–[8]. Efficient $\chi^{(2)}$ -based processes are essential for applications such as quantum light sources based on spontaneous parametric down-conversion (SPDC) [9] and metrology where SHG-based self-referencing is desired [10].

The strong light confinement of the AlGaAsOI waveguides enables dispersion engineering. It thus plays a crucial role in the implementation of modal phase matching (MPM) in the second harmonic generation (SHG), where different transverse spatial modes at the fundamental and second harmonic (SH) frequencies can be phase matched. Compared to conventional birefringent phase matching and quasi-phase matching methods, modal phase matching offers an approach to achieve high-efficiency SHG in waveguides. GaAs-on-insulator (GaAsOI) waveguides have been utilized to realize SHG with continuous-wave (CW) pumping at 2 μm [7]. Despite its high efficiency, GaAsOI waveguides are not suitable for SHG at the telecom wavelength (around 1.55 μm) because of the material bandgap. SHG with CW pumping at the telecom wavelengths has been demonstrated in suspended AlGaAs waveguides [8]. Although the reported high lossless normalized SHG efficiency shows the prospect of high-confinement AlGaAs waveguides in SHG, the obtained overall normalized efficiency is rather limited due to the large waveguide loss.

In this work, we employ MPM and type-I configuration to achieve SHG in AlGaAsOI waveguides using a CW pump in the telecom band. We experimentally present phase-matched waveguide dimensions for SHG for the AlGaAsOI platform. We obtained an overall normalized efficiency of 200% W^{-1} cm^{-2} in a 1-mm-long waveguide at the pump wavelength of 1587 nm. Our work shows the potential of the AlGaAsOI waveguides for efficient $\chi^{(2)}$-based frequency conversion processes.

2 Results

Figure. 1(a) illustrates the schematic drawing of the cross-section of an AlGaAsOI waveguide, and the white arrow indicates the crystal orientation. The pump and SH modes are selected as fundamental transverse electric mode (TE_{00}) and fundamental transverse magnetic mode (TM_{00}). First, we find the PM condition by calculating the

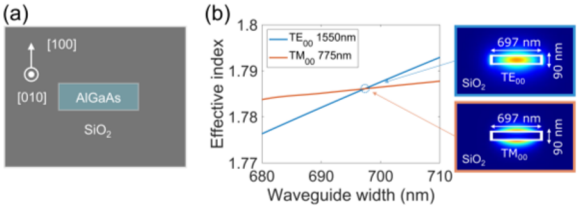

Fig. 1. (a) Cross-sectional schematic of the AlGaAsOI waveguide. (b) The effective index of the fundamental modes for waveguides with a thickness of 90 nm and varying widths. The blue and red lines represent the effective index of the TE_{00} mode at 1550 nm and the TM_{00} mode at 775 nm, respectively. (c) show the profiles of the fundamental modes (TE_{00} and TM_{00} modes) of the AlGaAsOI waveguide.

* Corresponding author: mipu@dtu.dk

effective indices of the fundamental and SH modes at different waveguide dimensions. A 90-nm-thick AlGaAs layer is required to obtain such an MPM condition. Fig. 1(b) shows the calculated effective index of TE_{00} mode at 1550 nm (blue) and TM_{00} mode at 775 nm (red) as a function of the waveguide width. The cross point, occurring at a width of 697 nm, corresponds to the PM condition. The mode profiles of the TE_{00} mode at 1550 nm and TM_{00} mode at 775 nm are shown in Fig. 1(c), which shows the optimal mode overlap between the pump and SH modes among all the different MPM conditions. Thanks to the high-confinement waveguide and large effective second-order nonlinear coefficient, an efficient SHG process is expected for the TE_{00}-TM_{00} MPM in the AlGaAsOI platform.

We fabricated 1-mm-long AlGaAsOI waveguides with different widths to find the PM wavelengths. The AlGaAsOI wafers were fabricated through wafer bonding and substrate removal process [11], [12]. The devices were patterned using electron-beam lithography and dry etching [13]. To characterize the SHG performance, we pump all the waveguides using a CW pump. The pump light polarization is adjusted to be coupled to the TE_{00} mode of the waveguide. Fig. 2(a) shows the normalized SHG spectra for different waveguide widths at room temperature. PM wavelengths shift from 1603 nm to 1548 nm as the waveguide width increases from 660 nm to 690 nm. The SHG bandwidth is measured as 15 nm to 6 nm. We attribute the large SHG bandwidth to the thickness uniformity along a 1-mm long waveguide as a 1-nm thickness variation corresponds to around 10-nm PM wavelength shifts [14].

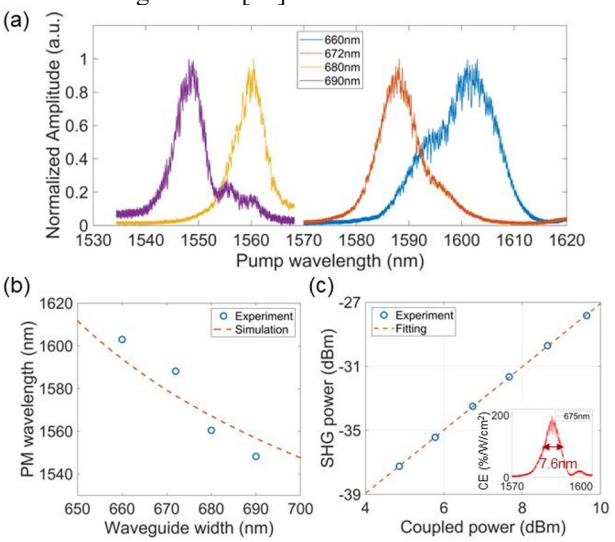

Fig. 2. (a) Measured spectra of SHG signal (normalized) as a function of the pump wavelength for AlGaAsOI waveguides with different widths. (b) Measured (blue circles) and calculated (dashed orange line) PM wavelength as a function of waveguide width. The waveguide height is around 90 nm. (c) Measured on-chip SHG power as a function of the coupled pump power in a 1-mm long straight waveguide with a width of 675 nm. Inset is the SHG spectrum of the measured waveguide.

Figure 2(b) plots the simulated PM wavelength as a function of waveguide width (dashed orange line). The solid blue circles are measured data, indicating a good agreement with the simulated results. We also measured the SHG power as a function of coupled pump power at the fixed pump wavelength of 1587.2 nm, as shown in Fig. 2(c). The extracted overall normalized conversion efficiency is 200% W^{-1} cm^{-2}. The obtained normalized CE is lower than previous works of SHG in GaAs at 2um pump wavelength [14]. One reason is the non-uniform AlGaAs layer thickness because of the much larger SHG bandwidth of 7.6 nm. It significantly compromises the SHG efficiency. Another possible reason is that the propagation loss at SH wavelengths, which is close to the bandgap of our AlGaAs (Al concentration of 21%), is significant. Therefore, it is crucial to improve the thickness uniformity of AlGaAsOI wafers further and reduce the waveguide propagation loss, especially at the SH frequencies.

3 Conclusion

In conclusion, we have demonstrated a simple approach to achieve efficient SHG through type-I MPM on the AlGaAsOI platform. We achieved an overall normalized conversion efficiency of 200% W^{-1} cm^{-2} in a single-pass 1-mm-long SHG device. Combining the $\chi^{(2)}$-based SHG with the $\chi^{(3)}$-based supercontinuum generation [15], one can realize octave-spanning comb generation and frequency doubling in the same platform, facilitating the miniaturization of self-referenced combs.

This work is supported by European Innovation Council (CSOC 101047289), European Research Council (REFOCUS 853522).

References

1. G. I. STEGEMAN et al., Journal of Nonlinear Optical Physics & Materials 03 347–371 (1994).
2. E. Mobini, D. H. G. Espinosa, K. Vyas, and K. Dolgaleva, Micromachines, 13. MDPI, 01-Jul-2022.
3. M. Pu, L. Ottaviano, E. Semenova, and K. Yvind, Optica 3 823 (2016).
4. M. Pu et al., Laser Photon Rev 1800111 (2018).
5. D. Kong et al., Nat Commun 13 4139 (2022).
6. L. Chang et al., Laser Photon Rev 12 1800149 (2018).
7. E. J. Stanton et al., Opt Express 28 9521 (2020).
8. I. Roland et al., Micromachines (Basel) 11 229 (2020).
9. F. Appas et al., Journal of Lightwave Technology 1–11 (2022).
10. Z. L. Newman et al., Optica 6 680 (2019).
11. L. Ottaviano, M. Pu, E. Semenova, and K. Yvind, Opt Lett 41 3996 (2016).
12. Y. Zheng, M. Pu, H. K. Sahoo, E. Semenova, and K. Yvind, Journal of Lightwave Technology 37 868–874 (2019).
13. C. Kim et al., IEEE Journal of Selected Topics in Quantum Electronics 29 1–13 (2022).
14. L. Chang et al., Laser Photon Rev 12 (2018).
15. B. Kuyken, M. Billet, F. Leo, K. Yvind, and M. Pu, Opt Lett 45 603 (2020).